Spontaneous network activity accounts for variability in stimulus-induced gamma responses

Jan Hirschmann[a], Sylvain Baillet[b], Mark Woolrich[c,d], Alfons Schnitzler[a,e], Diego Vidaurre[c,f] *, Esther Florin[a] *

*equal contribution

[a] Institute of Clinical Neuroscience and Medical Psychology, Medical Faculty, Heinrich Heine University, 40225 Düsseldorf, Germany

[b] McConnell Brain Imaging Centre, Montreal Neurological Institute, McGill University, Montréal, QC H3A2B4, Canada

[c] Wellcome Centre for Integrative Neuroimaging, Department of Psychiatry, Oxford Centre for Human Brain Activity (OHBA), University of Oxford, Oxford OX3 7JX, United Kingdom

[d] Wellcome Centre for Integrative Neuroimaging, Nuffield Department of Clinical Neurosciences, Oxford Centre for Functional MRI of the Brain (FMRIB), University of Oxford, Oxford OX3 9DU, United Kingdom

[e] Center for Movement Disorders and Neuromodulation, Department of Neurology, Medical Faculty, Heinrich Heine University, 40225 Düsseldorf, Germany

[f] Graduate School of Frontier Biosciences. Department of Brain Physiology, Osaka University, Osaka 565-0871, Japan

Abstract

Gamma range activity in human visual cortex is believed to play a major role in cognitive functions, such as selective attention. Although recent studies have revealed substantial variability in gamma activity, its origins are still unclear.

We investigated whether variability in stimulus-induced gamma activity is related to the spontaneous dynamics of resting-state networks using Hidden Markov Modelling. The magnetoencephalogram (MEG) of 15 healthy participants was recorded at rest and while they were performing a task involving a visual stimulus inducing strong, narrow-band gamma activity. Brain states were inferred from the task's baseline periods and from resting-state recordings, respectively.

Our results show how network states are related to the amplitude of stimulus-induced gamma responses. Across trials, we found an association between the amplitude of gamma responses and the brain state occurring immediately prior to stimulus presentation. Strong gamma responses followed a state characterized by prominent delta/theta oscillations in parieto-occipital regions and comparably weak alpha activity. Across subjects, the overall probability of visiting this state in the baseline period, i.e. the individual preference for this state, correlated positively with the amplitude of the trial-averaged gamma response. Remarkably, this relationship persisted when states were inferred from resting-state recordings rather than the task's baseline.

In summary, both within- and across-subject variability in stimulus-induced gamma activity can in part be explained by the ongoing dynamics of whole-brain network states. Fast, pre-stimulus modulations of brain states account for differences between trials while stable, individual state preferences account for differences between subjects.

Introduction

Narrow-band gamma activity has been observed in numerous species and brain areas with various recording techniques (1), including M/EEG recordings in humans (2). It has been proposed to play a role in a variety of cognitive processes, including attention (3, 4), feature binding (5, 6) , memory encoding (7, 8), memory retrieval (9, 10), decision-making (11, 12), and reward processing (13, 14).

Like any physiological response, stimulus-induced gamma activity varies within and between subjects. Within-subject variability of stimulus-induced gamma responses is substantial. Invasive recordings in monkeys (15) and humans (16) revealed that gamma responses vary markedly from trial to trial. Overall, single-trial gamma responses have been described as transient events of varying amplitude, duration and frequency, suggesting that the trial average, which resembles a continuous oscillation, does not capture the actual physiological processes engaged in single trials (17, 18). Although potentially misleading about the nature of gamma responses, averaging across trials results in a remarkably reproducible pattern within individuals, as shown by MEG studies measuring trial-average gamma responses in human visual cortex repeatedly in the same subjects (19, 20). Between subjects, in contrast, the trial-average response differs markedly with respect to amplitude, frequency and bandwidth (20) and this between-subject variability has been shown to have a relatively strong genetic basis (21).

The most common approach to studying gamma-band activity in humans is to compare trial- or subject-averages across experimental conditions (e.g. 22, 23). In this framework, within- and between-subject variability is usually not a parameter of interest. The present study, in contrast, focuses on the variability of gamma responses and how it may be related to ongoing network activity immediately prior to stimulus onset and in the resting-state (before/after task performance). We aimed at answering two major research questions. The first question, relating to variability across trials, is whether the strength of the gamma response depends on the network state immediately preceding stimulus onset. In other words, could gamma responses differ across trials because the pre-stimulus brain state varies from trial to trial? Previous M/EEG studies have already revealed an influence of pre-stimulus oscillations (typically, ≤ 1s before stimulus onset) on behavioural performance in perception tasks (24–26), suggesting that a similar influence might be exerted on stimulus-induced brain responses. The second question, relating to variability across subjects, is whether the amplitude of the trial-average gamma response is related to individual phenotypes of network dynamics. In other words, do individuals differ in their gamma response because some subjects spend more time in certain network states than others? Unlike the first question, the latter does not address the immediate, pre-stimulus period, but temporally stable features of whole-brain network activity. Similar stable features of network activity have been found to predict stimulus-induced brain responses in functional magnetic resonance (fMRI) studies (27, 28).Here, we sought to find neurophysiological correlates at higher temporal resolution using MEG imaging.

In contrast to previous M/EEG studies, we did not restrict our analysis to a specific brain area or frequency band; instead, we studied network activity in a wide frequency range (1-35 Hz) with Hidden Markov Models (HMMs). HMMs are probabilistic sequence models that specialise in finding recurring patterns in multivariate data (29). Unlike sliding-window approaches, they can reveal fast state changes present in multichannel, electrophysiological recordings (30–33). HMMs describe the dynamics of brain activity as a sequence of transient events, each of which corresponds to a visit to a particular brain state. For each state, the HMM infers a time-course that describes the probability of

that state being active. Furthermore, each state is characterized by a unique spatio-spectral profile. In summary, HMM brain states can be considered a compact description of multi-faceted, recurring patterns in dynamic network activity. HMMs have been widely used in a variety of applications, such as the decoding of speech (34), the comparison of nucleotide sequences (35) or the detection of pathological brain signals (36).

The paradigm and rationale of the present study are illustrated in Fig. 1. In short, MEG data were acquired from 15 healthy participants while they performed a reaction time task. Subjects were presented with an inward-moving, circular sine wave grating, known to induce strong gamma activity in visual cortex (19). They were instructed to press a button as soon as they detected an increase in grating speed. In addition, two resting-state MEG measurements were obtained: one before and one after the task. Whole-brain network states were derived from 1-35 Hz ongoing activity in 1) the pre-stimulus task baseline and 2) the resting-state recordings. The restriction to spontaneous sub-gamma activity was made to prevent the detection of trivial relationships between pre- and post-stimulus gamma activity (see Materials and Methods).

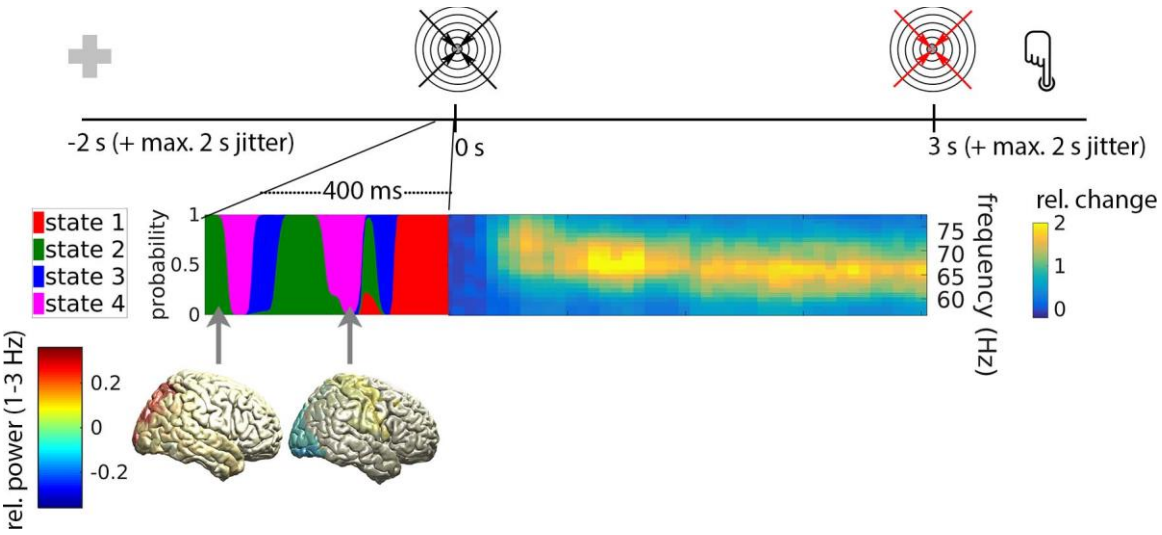

Fig. 1: *Experimental paradigm and rationale of the study*. Upper row: Timeline of a single trial, locked to grating onset. Following a baseline period of 2 to 4 s with a central fixation cross, an inward-moving grating appeared which accelerated at an unpredictable moment 3 to 5 s following grating onset (illustrated here with red arrows). Subjects indicated they detected the acceleration via button press. Lower left: Hidden Markov Modelling yielded at each time sample the probability of the brain being in any of four states (color-coded). State inference was limited to epochs without stimulation, i.e. to the pre-stimulus baseline, as shown here, or to the resting-state (not shown). Each state is characterized by a unique spatio-spectral profile within the frequency ranges slower than gamma (1-35 Hz), including the topography of delta power shown here for states 2 (left) and 4 (right). Lower right: The inward-moving grating induced strong gamma activity in occipital areas. We investigated whether the strength of this stimulus-induced gamma response is related to spontaneously occurring whole-brain states.

Results

State properties

We assessed the spectral and temporal profile of four states derived from the baseline periods of the task. Whereas it is possible to describe the data using more states, four were adequate for our purposes (justified in Materials and Methods). Fig. 2A shows the power and coherence spectra associated with each state. Although all state spectra were dominated by parieto-occipital alpha peaks, baseline states differed with respect to multiple spectral features.

We investigated the temporal properties of these baseline states. The smallest number of visits for any state-subject combination was 338, i.e. all subjects visited all states repeatedly in the baseline period. On average, a state visit lasted 106 ms. This average lifetime defined the pre-stimulus time window of interest (-106 to 0 ms), which was designed to capture the state last visited before the appearance of the moving grating. Fig. S1 describes additional, time-average state properties.

We next investigated how the state probabilities estimated by the HMM evolved in the baseline period of the task. To this end, we averaged the state probabilities, time-locked to the beginning of the baseline period (fixation-cross onset), across trials. The resulting average, referred to as fractional occupancy (FO), quantifies how often a given state occurred at each point in the baseline period (30). Although HMM inference was performed without providing explicit information about the timing of the experiment, FO changed systematically as stimulus presentation approached, suggesting an effect of stimulus anticipation (Fig. 2B). State 1 was found to be predominant early in the baseline, but its FO decreased over time (mean slope = -0.065, $p < 0.001$; *t*-test). State 2's FO increased over time (mean slope = 0.086, $p < 0.001$; *t*-test). The FO of state 3 showed a weak negative dependency on time (mean slope = -0.020, $p = 0.02$; *t*-test) and state 4's FO did not change significantly (mean slope = -0.001, $p = 0.87$; *t*-test). We verified that FO was independent of heartbeat and eye blinks (Fig. S2).

Gamma responses and pre-stimulus network state

Next, we investigated whether the spontaneous occurrence of whole-brain network states immediately before grating onset can account for within-subject, trial-to-trial variability of induced gamma responses. As depicted in Fig.1, the HMM provided a probability for each state at each time point in the baseline period. We averaged these probabilities across the pre-stimulus time window of interest (-106 to 0 ms) and used the average probabilities as weights for the computation of state-specific, weighted trial-averages. This procedure can be considered a soft-assigned, within-subject grouping of trials by pre-stimulus state. Subsequently, we tested whether the resulting state-specific trial averages differed with respect to post-stimulus gamma amplitude. Note that such differences may only occur if there is quantitative relationship between pre-stimulus state and post-stimulus gamma amplitude, since trials were grouped by the former.

As depicted in Fig. 2C, the amplitude of stimulus-induced gamma activity differed across pre-stimulus states ($p = 0.013$; Friedman test). Post-hoc comparisons revealed that baseline state 2 was associated with stronger stimulus-induced gamma activity than baseline state 4 ($p = 0.004$; Wilcoxon rank-sum test). This pattern was seen in most individual subjects (Fig. S3) and was not biased by the trial-weighting procedure (Supplementary Material). These results demonstrate that state switching in

the baseline period can explain part of the within-subject variability in stimulus-induced gamma responses.

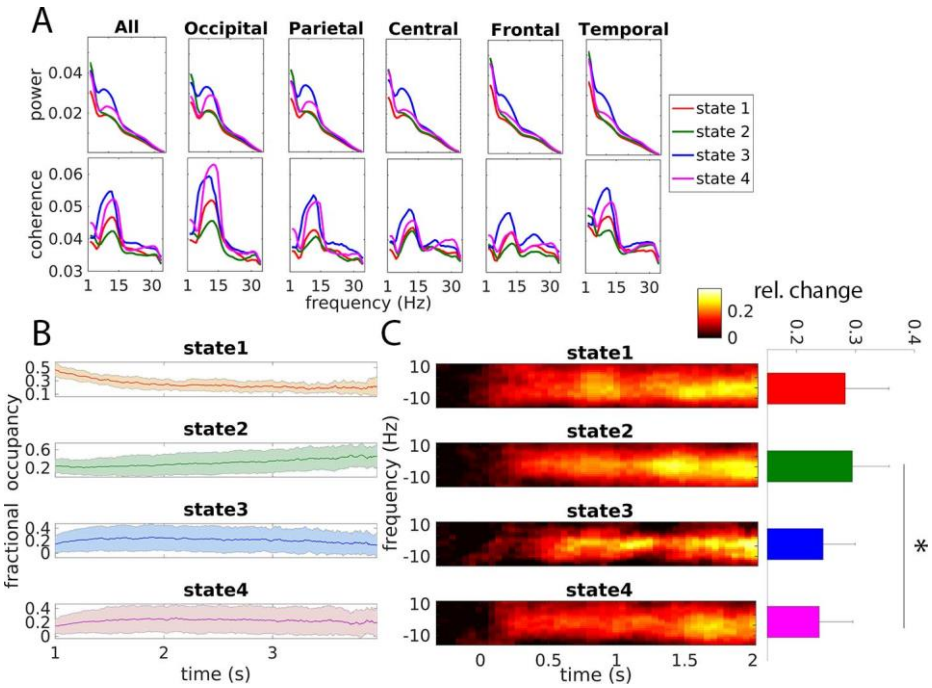

Fig. 2: *Relationship between gamma responses and pre-stimulus network state*. **A)** Power (upper row) and coherence spectra (lower row) for each of the four baseline states, averaged over all, occipital, parietal, central, frontal and temporal brain regions, respectively**. B)** Fractional occupancy in the baseline period (1-4 s before grating onset), averaged over subjects and time-locked to the onset of the fixation cross. Shaded areas indicate the standard deviation over subjects. The first second of each trial was discarded to reduce the effect of movement-related processing occurring after the button press. **C)** Left: Weighted average time-frequency representations of gamma responses, time-locked to the appearance of the moving grating. 0 Hz marks individual gamma-peak frequency (between 42 and 74 Hz). Power was baseline-corrected (-0.5 to -0.2 s from grating onset). Right: Power averaged over frequency (individual gamma peak frequency ±10 Hz) and time (0.6 to 2s).

Gamma responses and individual state preferences

To investigate the contribution of baseline states to inter-subject variability, we correlated the power of the trial-averaged, stimulus-induced gamma response with the mean state probability in the entire baseline period of the trial (from 1 to max. 3 s relative to fixation-cross onset; Fig 1). We found that the probability of being in baseline state 2 (the state that elicited strong oscillatory responses within subjects) was positively correlated with trial-averaged gamma power (r = 0.690, p = 0.004), i.e. subjects spending more time in baseline state 2 tended to exhibit stronger stimulus-induced gamma activity on average. The other states showed a weaker, negative correlation (state 1: r = -0.57, state 3: r = -0.32, state 4: r = -0.41). These results demonstrate that state preferences in the baseline period can explain between-subject variability in stimulus-induced gamma activity.

To investigate the link between the amplitude of stimulus-induced gamma activity and resting-state activity, we re-ran the HMM inference on the resting-state recordings preceding and following the

task, respectively. The three recordings (rest-pre, task, and rest-post) were recorded in direct succession in most subjects (see Materials and Methods). For both resting-state recordings, we identified a state reminiscent of baseline state 2, characterized by strong power between 1 and 5 Hz and the lack of an alpha peak in the region-average power spectrum (Fig. 3A). Topographically, the 1-5 Hz peak mapped to bilateral parietal and sensorimotor cortices (Fig. 3B). Similar to the baseline periods (r = 0.690), the probability of being in the high delta/low alpha state at rest was positively correlated with trial-averaged, stimulus-induced gamma power (rest-pre: r = 0.700, p = 0.005; rest-post: r = 0.538, p = 0.046), i.e. subjects spending more time in this state at rest tended to show stronger gamma activity in the task (Fig. 3C). This persisting correlation demonstrates that time-average state probabilities reflect individual state preferences which are stable across several hours and across experimental conditions (cf. Fig. S4).

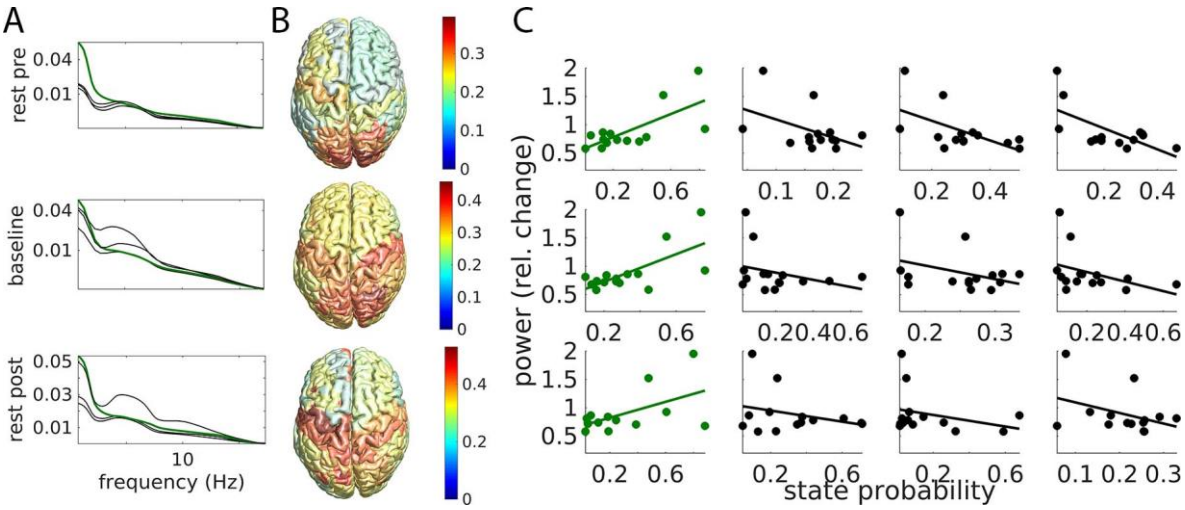

Fig. 3: ***Relationship between gamma responses and individual state preferences.*** **A**: Power spectra averaged over parcels for all four states in the resting-state recording preceding the task (top), the task's baseline periods (middle), and in the resting-state recording following the task (bottom). A state characterized by strong delta/theta oscillations and comparatively weak alpha oscillations was observed in all recordings (marked in green). **B**: Spatial distribution of power between 1 and 5 Hz, relative to the mean over all rest-pre, baseline, and rest-post states. **C**: Across-subject correlation between the amplitude of stimulus-induced gamma activity and time-average state probability. Each state is represented by one plot within each row. Within each row, states are sorted by correlation coefficient from left to right in descending order. Note that, with the exception of the first column, states are not matched across rows (recordings), i.e. states within a column might differ with respect to power and coherence.

The gamma-enhancing network state

Our observations suggest the existence of a whole-brain state with an enhancing effect on gamma responses occurring both at rest and in the baseline period of a task. To further characterize this state, we maximized the amount of available information by concatenating the data and the state probabilities from the baseline periods and the two resting state recordings, and we computed the topography of power and coherence in this state (Fig. 4). The gamma-enhancing network state

exhibited strong delta/theta power in central parieto-occipital regions and sensorimotor cortex, as well as weak alpha power in all areas posterior to the central sulcus and in the temporal lobes. The spatial distribution of power was remarkably symmetric with respect to the interhemispheric fissure. The topography of coherence was similar to the topography of power in the alpha and beta band, but deviated at lower frequencies. Delta coherence, in particular, was high in left primary somatosensory cortex.

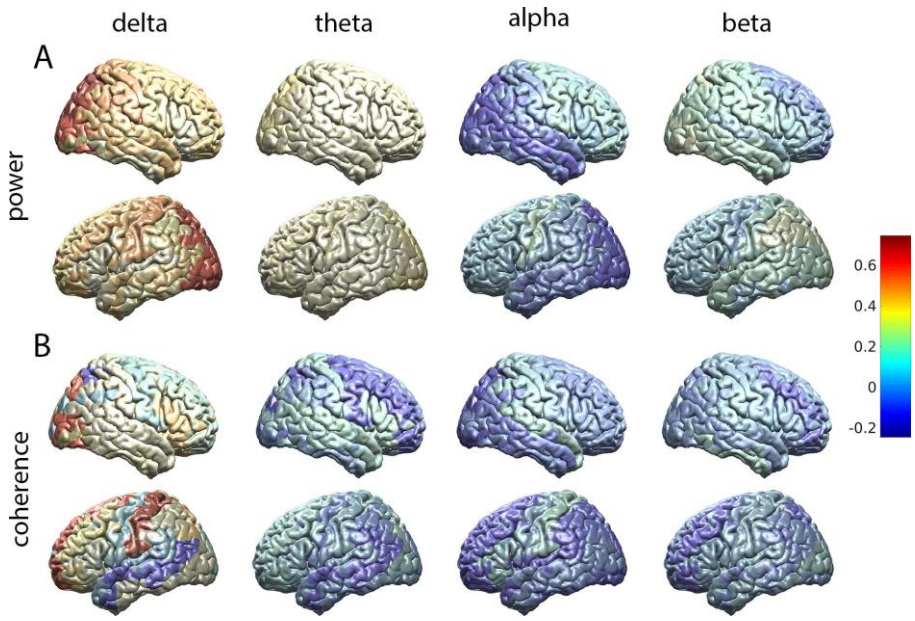

Fig. 4: *Characterization of the gamma-enhancing network state.* Columns from left to right: delta (1-4 Hz), theta (5-7 Hz), alpha (8-12 Hz) and beta (13-35 Hz). **A)** Power relative to the mean across states. **B**) Coherence relative to the mean across states. Colours indicate the average coherence of each parcel with all other parcels, relative to the mean across states.

Low posterior alpha power does not explain strong gamma responses

We considered the possibility that the gamma-enhancing network state owes its gamma-enhancing properties solely to low pre-stimulus alpha power in parieto-occipital cortex. To explore this possibility, we split the trials into two groups based on alpha power observed in the cuneus over the last 106 ms before stimulus onset (lower 50% vs. higher 50%). Stimulus-induced gamma power did not differ between these groups within subjects (p = 0.43; Friedman test) and pre-stimulus alpha power did not correlate with stimulus-induced gamma power across subjects (r = 0.008, p = 0.974). Similar results were obtained when comparing three levels of alpha power and when considering all parieto-occipital brain areas instead of only the cuneus (data not shown). These results suggest that low parieto-occipital alpha power does not fully explain the enhancement the gamma response, highlighting the relevance of spontaneous network dynamics provided by the HMM.

Discussion

We have demonstrated that spontaneously occurring network states account for within- and between-subject variability in stimulus-induced gamma activity. In particular, we have provided evidence for a network state favouring strong gamma responses of visual cortex to an inward-moving grating. Stimulus-induced gamma activity was stronger when this state preceded stimulus onset on a

given trial. Further, stimulus-induced gamma activity was stronger in subjects visiting this state frequently during the baseline periods of the task or during rest.

The effect of pre-stimulus oscillations on induced gamma activity

An important insight from this study is that stimulus-induced gamma activity is related to pre-stimulus states derived from activity between 1 and 35 Hz, suggesting that the gamma response depends on slower, pre-stimulus oscillations. These results are in agreement with a recent MEG study demonstrating that post-stimulus gamma lateralization in response to a spatial cue is correlated with pre-stimulus alpha lateralization (37). The authors further showed that the phase of alpha oscillations modulates the amplitude of gamma activity in the pre-stimulus period and that alpha activity in visual cortex is driven by the frontal eye field. Their results support a general framework for inter-area communication, in which gamma activity mediates bottom-up communication and alpha/beta oscillations are markers of top-down influences (38–40). Such frequency-specific communication is believed to enable fundamental aspects of human perception, such as spatial attention, and indeed, both alpha and gamma activity are strongly modulated by attention (41–44). Although our findings argue against alpha as an exclusive mediator of pre-stimulus effects in this paradigm (see below), it is conceivable that brain state dynamics in the baseline period reflect dynamic modulation of attention, mediated by concerted oscillations below 35 Hz.

Network vs. local activity

A crucial feature of our approach is that it allows for relating network activity, rather than local activity, to visual processing. This is achieved by the use of Hidden Markov Modelling, which models the activity of all sources simultaneously and can fully leverage the high temporal resolution of electrophysiological data. Recent MEG studies using HMMs revealed a rich repertoire of fast-changing network states characterized by distinct topographies of spectral power and coupling, many of which were reminiscent of the resting-state networks originally obtained with fMRI (30–33). HMMs and other whole-brain models have also been applied to describe dynamic connectivity in fMRI data (45, 46).

The ability to investigate network activity allowed a more complete description of spontaneous activity in relation to stimulus processing. Given the highly-interconnected structure of the brain, it is unlikely for the local processes serving the gating of sensory information (such as the modulation of posterior alpha power) to work in isolation. In line with this assumption, we have shown that low posterior alpha power is a major feature of the gamma-enhancing network state, but is in itself not sufficient to explain the predisposition for strong gamma responses.

Spontaneous activity is correlated with stimulus-induced activity

We found an association between stimulus-induced gamma activity and network states occurring in the absence of a stimulus, implying that spontaneous activity could predict individual stimulus-induced responses. This is in agreement with a number of fMRI studies demonstrating interactions between resting-state and task-related activity (47). Resting-state and task-related networks were found to be highly similar across a wide variety of tasks (48, 49). Furthermore, stimulus-induced patterns of activation could be predicted from resting-state activity (27, 28). These studies suggest that task-related activity arises by relatively minor modulations of the basic functional connectome, which was demonstrated to be a robust, individual trait, allowing for accurate identification of individual subjects (50). Neurophysiological activity has seldom been investigated in this context; we

only know of one electrocorticography study in non-human primates reporting high similarity between resting-state and stimulus-induced neuronal activity in visual cortex (51).

While fMRI studies on spontaneous activity have mostly, but not exclusively (48, 49), addressed the resting-state, electrophysiological studies in humans have related brain activity occurring immediately before stimulus onset (≤ 1s) to perception. Pre-stimulus alpha and beta oscillatory activity, for example, were found to bias the perception of briefly presented or difficult-to-distinguish visual (24, 54, 55) and tactile stimuli (56–59). Unlike resting-state networks, which are usually obtained by collapsing activity over time and thus emphasize stable configurations of brain activity, pre-stimulus activity is believed to reflect processes that vary on a trial-by-trial basis, such as attention and/or stimulus anticipation (43).

In this study, we have assessed the relationship of both pre-stimulus *and* resting-state activity with stimulus-induced gamma activity. Pre-stimulus brain states were found to affect the amplitude of gamma responses within subjects, suggesting that the dynamics of pre-stimulus brain states reflect fast-changing internal processes distinguishing between trials, such as the level of anticipation. An anticipatory effect is further supported by the fact that state probabilities underwent systematic modulations as stimulus onset approached (Fig. 2).

When considering state probabilities averaged over the entire baseline period rather than the immediate, pre-stimulus interval, we found that the overall fraction of time spent in the state preceding strong gamma responses correlated positively with the amplitude of the individual, trial-average gamma response. Thus, the same brain state, referred to as the gamma-enhancing network state, predicted strong responses within and across subjects. Note that such correspondence between trial- and subject-level is not unexpected, since spending a lot of time in a gamma-enhancing network state increases the probability of responding strongly to stimulus onset in any given trial, thus favoring a strong average response. It is, however, a good indicator that the reported subject-level correlations are not driven by outliers. While it is possible that any brain state is overrepresented in strong responders by chance, it is very unlikely that the same state enhances gamma responses within these subjects (trial-level). Conversely, differences arising by chance within subjects are not expected to translate into a relationship across subjects.

A state very similar to the gamma-enhancing network state observed at baseline was found in the resting-state recordings. Again, the individual preference for this state correlated with the individual gamma response. These observations suggest that the general preference for the gamma-enhancing network state is an individual characteristic that can be estimated from any recording containing spontaneous activity, irrespective of context and time. Provided that future studies confirm its robustness and predictive power in other settings, the probability of visiting the gamma-enhancing network state might turn out to be a highly informative and compact feature of the individual functional connectome, summarizing key aspects in a single number.

Limitations

While this work demonstrates a correlation between resting-state activity and brain responses, it does not attempt to predict brain responses form resting-state activity, as performed in previous fMRI studies (27, 28). Making detailed predictions about multiple response parameters, including frequency band and spatial distribution, in a wide variety of tasks will be an important challenge for future studies.

Another limitation of this study is that it does not relate brain states to behaviour. While the paradigm did involve the measurement of reaction time, we found the variability of reaction times to be unusually large, most likely because subjects occasionally missed the acceleration of the moving spiral and simply pressed the button after a waiting period. An investigation of this matter would require a different paradigm with a more reliable assessment of behaviour.

Furthermore, due to the use of Principal Component Analysis for dimensionality reduction, the method applied here biases the state decomposition towards slow, high-amplitude oscillations (33). Hence, faster rhythms such as beta oscillations are possibly underrepresented, whereas delta and theta oscillations dominate state inference. Future work will be necessary to find similar effects in higher bands.

Conclusions

We have shown that within- and across-subject variability in stimulus-induced gamma activity can in part be explained by brain state dynamics. Spontaneously occurring brain states reflect both fast-changing factors distinguishing between trials and temporally stable factors distinguishing between subjects.

Material and Methods

Participants

15 healthy participants were recruited for this study (21-45 years; 5 female). The study was approved by the Montreal Neurological Institute's ethics committee (NEU 011-036) and was in accordance with the Declaration of Helsinki. All participants gave written informed consent and were compensated for their participation.

Paradigm

Subjects were presented with a modified version of the visual stimulation paradigm by Hoogenboom et al. (19): An inward-moving, circular sine wave grating with a diameter of 5° accelerated from 1.6 deg/s to 2.2 deg/s at an unpredictable moment between 3-5 seconds after stimulus onset. Subjects indicated that they detected the velocity change by pressing a button with the index finger of the dominant hand. The button press ended the trial and the stimulus was turned off. During the inter-trial interval (baseline period), subjects were presented with a central fixation cross. Inter-trial intervals varied between 2 and 4s. A few trials with longer interval (17 - 19 s) were randomly interspersed in the trial sequence for all subjects but P1 (6 - 16 per subject; mean: 13). This was done to facilitate an analysis of the influence of baseline duration, but is not relevant for the analyses reported here.

Experimental Procedure

Each session started with a 5 min resting-state recording with eyes open, which was immediately followed by task practice and recording. Before the start of the reaction time task, participants completed 10 practice trials. The task was divided into 2 - 5 blocks, containing 35 - 78 trials each (mean: 62.85). After each block, participants received a feedback on the accuracy of their responses and had the possibility to take a break. Following the reaction time task, a further 5 min resting-state recording was acquired.

In two subjects (P3 and S006R), additional task data were acquired 6 days and 1 day after the first recording session, respectively. Subject P1 was not recorded in resting state.

Data acquisition

Participants were measured in a seated position with a 275-channel VSM/CTF MEG system at a sampling rate of 2400 Hz (no high-pass filter, 660 Hz anti-aliasing online low-pass filter). Electrocardiography (ECG) and vertical electrooculography (EOG) were recorded simultaneously using MEG-compatible electrodes. Magnetic shielding was provided by a magnetically-shielded room with full 3-layer passive shielding. Participant preparation consisted of affixing 3 head-positioning coils to the nasion and both pre-auricular points. The position of the coils relative to the participant's head was measured using a 3-D digitizer system (Polhemus Isotrack, Colchester, USA).

A T1-weighted MRI of the brain (1.5 T, 240 x 240 mm field of view, 1 mm isotropic, sagittal orientation) was obtained from each participant either at least one month before or immediately after the session. In case the MRI was obtained before the MEG, a waiting period of 1 month was adhered to in order to prevent potential magnetic contamination.

Preprocessing

Data were preprocessed and analysed using the HMM-MAR (27, 28)[*] and Fieldtrip (60)[†] toolboxes for Matlab (The Mathworks). All data were screened visually. Noisy channels and noisy epochs were excluded from analysis. Data were down-sampled to 250 Hz. A 60 Hz discrete Fourier transform filter was applied to remove line noise. Cardiac and eye movement artefacts were isolated by FASTICA (61) and removed in non-automatic component selection.

Source reconstruction

Individual T1-weighted MR scans were aligned to the MEG's coordinate system, segmented and used for the construction of a single-shell, realistic head model (62). To define a set of source coordinates, the "colin27" template MRI (63) was inflated using FreeSurfer (64) and a cortical mesh consisting of 2052 sources was constructed using MNE (65). The corresponding coordinates in individual head space were obtained by applying the inverse of the normalizing transform matching the individual to the template MR scan. The lead field (forward model) was computed based on the source coordinates and the head model. Subsequently, a Linearly Constrained Minimum Variance (LCMV) spatial filter (66) was computed based on the lead field and the sensor covariance matrix, and data were projected through this filter trial-by-trial. Note that the sign of the beamformer output is arbitrary. Because our analysis requires sign consistency across subjects, we applied a sign flipping procedure to maximize sign consistency; see (31) and (33) for details.

To reduce dimensionality, we grouped sources into parcels, defined by the Talairach Tournoux atlas (52), and carried out all subsequent analyses on the parcel level. First, each source was either assigned to one of 25 bilateral brain areas of interest or discarded from further analysis if it was more than 5 mm away from an area of interest (325 of 2052 sources). The areas of interest consisted of all cortical areas contained in the atlas, with the exception of seven areas at the base of the brain or deep within the interhemispheric fissure, which were assumed to have poor MEG signal quality

[*] https://github.com/OHBA-analysis/HMM-MAR
[†] http://www.fieldtriptoolbox.org

(rectal gyrus, parahippocampal gyrus, subcallosal gyrus, transverse temporal gyrus, orbital gyrus, and uncus). The 25 bilateral brain areas of interest were further sub-divided into a left- and a right-hemispheric parcel, resulting in 50 cortical parcels of interest (Tab. 1 of the Supplementary Material). The first principle component was extracted from each parcel of interest and magnetic field spread between parcels was reduced by symmetric, multivariate orthogonalization (68).

Stimulus-induced gamma activity

We quantified post-stimulus gamma responses in order to relate them to brain states inferred from slower activity (≤35 Hz) occurring in the pre-stimulus baseline period or the resting-state recordings. Post-stimulus gamma responses were computed by multitaper spectral estimation using 2 Slepian tapers (69). Power was estimated for frequencies between 40 Hz and 100 Hz in a 300 ms sliding window which was moved in steps of 50 ms. We screened post-stimulus parcel activity and identified a frequency band, a time window and a location of interest. Because individual gamma peak frequencies varied markedly across subjects (between 42 and 74 Hz), frequency selection was subject-specific, i.e. we defined an individual gamma band for each subject (individual gamma peak frequency ±10 Hz). The time window of interest was set to 0.6 to 2 s relative to stimulus onset because all subjects were found to exhibit stable gamma activity in this window. The bilateral cunei were chosen as the locations of interest because this was generally the area with the strongest gamma response. For the analyses described in the following, gamma power within ±10 Hz of individual gamma peak frequency was normalized frequency-by-frequency by computing the percent change relative to mean power in the response baseline (-0.5 to -0.2 ms from grating onset) and averaged over frequency, time and locations of interest.

State inference

We selected either the baseline periods of the task, the rest recording preceding the task, or the rest recording following the task for state inference. In case the baseline period was selected, the first second of each trial was removed because it was assumed to contain activity related to the button press of the previous trial. Next, we *z*-scored and concatenated the data from all subjects in time, resulting in a total of 71.44 min of pre-task rest data (per subject mean: 5.10 min, STD: 1.40 min), 164.85 min of baseline data (per subject mean: 10.99 min, STD: 2.19 min) and 63.47 min of post-task rest data (per subject mean: 4.53 min, STD: 0.69 min). Importantly, we applied a spectral filter with a pass-band of 1 to 35 Hz to ensure that brain states were not based on gamma activity, which might lead to trivial relationships between brain states and gamma responses. For example, without such filtering, a baseline state might be characterized by strong gamma activity. Stimulus-induced, relative increases of gamma amplitude following this state might be low because the gamma amplitude cannot increase much further (ceiling effect).

State inference was performed by applying a Hidden Markov Model (HMM, 25), which was fitted to the data using stochastic variational inference (32). The HMM assigns one set of state probabilities (one probability for each state) to each sample of the multi-channel recording, while simultaneously estimating the parameters of each state from the data. Here, we used a variety of the HMM designed to capture transient patterns of power and phase-coupling, referred to as Time-delay Embedded HMM (TDE-HMM; 33). In this model, each state is characterized by the cross-correlations within a certain window of interest, implicitly containing spectrally-defined patterns of power and phase-coupling. Following (33), the length of the window was chosen to be 15 samples (60ms). As the

resulting embedded space is very high-dimensional, Principal Component Analysis was used to reduce dimensionality to 100, i.e. twice the number of parcels.

Similar to the frequency resolution in spectral analysis, the number of states *K* in a HMM determines the level of detail of the solution. As this study distributed trials across states (see below), we set *K*=4 to guarantee a reasonable amount of trials per state. Similar results were obtained for *K*=3.

State properties

Following state inference, we computed the power and coherence associated with each state as detailed in (31). In short, source activity was weighted by state probability before spectral estimation was performed using a multitaper approach, resulting in Fourier coefficients for each parcel and state. These coefficients were used for the computation of power and coherence. For topographic illustrations, power and coherence were interpolated on a 3D-reconstruction of the template brain after computing the relative difference with respect to the mean over states. In case of coherence, we display the average coupling with all other parcels.

For analyses involving fractional occupancy, we first determined the current state for each point in time by selecting the state with maximum posterior probability (posterior decoding). Subsequently, we computed the fraction of time spent in each state. Linear trends in fractional occupancy were revealed for each subject by linear regression analysis and regression coefficients were tested for consistent deviations from 0 using a one-sample *t*-test.

Analysis of within-subject variability

We hypothesized that the strength of stimulus-induced gamma activity depends on the network state immediately before stimulus presentation (Fig. 1). To test this, we first computed for each state the average state probability in the pre-stimulus time window of interest (-106 to 0 ms), which served as state-specific trial weight. Subsequently, we computed a weighted trial average for each state using these weights. This procedure can therefore be considered a weighted (soft-assigned), within-subject grouping of trials by pre-stimulus state. Next, we tested whether the resulting trial groups consistently differed in post-stimulus gamma amplitude across subjects. This was achieved by running a Friedman test, followed by post-hoc Wilcoxon rank sum tests. Note that trials were grouped by pre-stimulus state, not post-stimulus gamma amplitude, i.e. any consistent difference in gamma amplitude must be due to a relationship between pre-stimulus state and post-stimulus gamma amplitude.

Analysis of between-subject variability

We also assessed whether the amplitude of trial-averaged, stimulus-induced gamma responses is related to state preferences in the baseline periods of the task and/or the rest recordings preceding and following the task. State probabilities were averaged across the entire baseline/rest recording and tested for a linear correlation with the amplitude of the trial-averaged gamma response using a significance test for Pearson's correlation coefficient (Matlab function *corrcoef*). Note that a strong correlation with any of the states will induce a correlation of opposite sign with the remaining states, given that the states are mutually exclusive.

Acknowledgments

The Wellcome Centre for Integrative Neuroimaging is supported by core funding from the Wellcome Trust (203139/Z/16/Z). DV is supported by a Wellcome Trust Strategic Award (098369/Z/12/ Z). MWW is supported by the Wellcome Trust (106183/Z/14/Z) and the MRC UK MEG Partnership Grant (MR/K005464/1). SB was supported by a Discovery Grant from the Natural Science and Engineering Research Council of Canada (436355-13), the NIH (1R01EB026299-01) and a Platform Support Grant from the Brain Canada Foundation (PSG15-3755). EF is supported by the Volkswagen Foundation (Lichtenberg program 89387).

References

1. Bosman CA, Lansink CS, Pennartz CMA (2014) Functions of gamma-band synchronization in cognition: from single circuits to functional diversity across cortical and subcortical systems. *Eur J Neurosci* 39(11):1982–1999.

2. Jensen O, Kaiser J, Lachaux J-P (2007) Human gamma-frequency oscillations associated with attention and memory. *Trends Neurosci* 30(7):317–324.

3. Bosman CA, et al. (2012) Attentional Stimulus Selection through Selective Synchronization between Monkey Visual Areas. *Neuron* 75(5):875–888.

4. Grothe I, Neitzel SD, Mandon S, Kreiter AK (2012) Switching Neuronal Inputs by Differential Modulations of Gamma-Band Phase-Coherence. *J Neurosci* 32(46):16172–16180.

5. Engel AK, Konig P, Kreiter AK, Singer W (1991) Interhemispheric synchronization of oscillatory neuronal responses in cat visual cortex. *Science (80-)* 252(5010):1177–1179.

6. Singer W, Gray C (1995) Visual feature integration and the temporal correlation hypothesis. *Annu Rev Neurosci* 18:555–586.

7. Sederberg PB, Kahana MJ, Howard MW, Donner EJ, Madsen JR (2003) Theta and gamma oscillations during encoding predict subsequent recall. *J Neurosci* 23(34):10809–10814.

8. Jutras MJ, Fries P, Buffalo EA (2009) Gamma-Band Synchronization in the Macaque Hippocampus and Memory Formation. *J Neurosci* 29(40):12521–12531.

9. Montgomery SM, Buzsaki G (2007) Gamma oscillations dynamically couple hippocampal CA3 and CA1 regions during memory task performance. *Proc Natl Acad Sci* 104(36):14495–14500.

10. Osipova D, et al. (2006) Theta and Gamma Oscillations Predict Encoding and Retrieval of Declarative Memory. *J Neurosci* 26(28):7523–7531.

11. van Wingerden M, Vinck M, Lankelma J V., Pennartz CMA (2010) Learning-Associated Gamma-Band Phase-Locking of Action-Outcome Selective Neurons in Orbitofrontal Cortex. *J Neurosci* 30(30):10025–10038.

12. van Wingerden M, van der Meij R, Kalenscher T, Maris E, Pennartz CMA (2014) Phase-Amplitude Coupling in Rat Orbitofrontal Cortex Discriminates between Correct and Incorrect Decisions during Associative Learning. *J Neurosci* 34(2):493–505.

13. Kalenscher T, Lansink CS, Lankelma J V., Pennartz CMA (2010) Reward-Associated Gamma Oscillations in Ventral Striatum Are Regionally Differentiated and Modulate Local Firing Activity. *J Neurophysiol* 103(3):1658–1672.

14. Berke JD (2009) Fast oscillations in cortical-striatal networks switch frequency following rewarding events and stimulant drugs. *Eur J Neurosci* 30(5):848–859.

15. Lundqvist M, et al. (2016) Gamma and Beta Bursts Underlie Working Memory. *Neuron* 90(1):152–164.

16. Kucewicz MT, et al. (2014) High frequency oscillations are associated with cognitive processing in human recognition memory. *Brain* 137(8):2231–2244.

17. Jones SR (2016) When brain rhythms aren't "rhythmic": implication for their mechanisms and meaning. *Curr Opin Neurobiol* 40:72–80.

18. van Ede F, Quinn AJ, Woolrich MW, Nobre AC (2018) Neural Oscillations: Sustained Rhythms or Transient Burst-Events? *Trends Neurosci*. doi:10.1016/J.TINS.2018.04.004.

19. Hoogenboom N, Schoffelen JM, Oostenveld R, Parkes LM, Fries P (2006) Localizing human visual gamma-band activity in frequency, time and space. *Neuroimage* 29(3):764–773.

20. Muthukumaraswamy SD, Singh KD, Swettenham JB, Jones DK (2010) Visual gamma oscillations and evoked responses: Variability, repeatability and structural MRI correlates. *Neuroimage* 49(4):3349–3357.

21. van Pelt S, Boomsma DI, Fries P (2012) Magnetoencephalography in twins reveals a strong genetic determination of the peak frequency of visually induced γ-band synchronization. *J Neurosci* 32(10):3388–92.

22. Bauer M (2006) Tactile Spatial Attention Enhances Gamma-Band Activity in Somatosensory Cortex and Reduces Low-Frequency Activity in Parieto-Occipital Areas. *J Neurosci* 26(2):490–501.

23. Muthukumaraswamy SD, Singh KD (2013) Visual gamma oscillations: The effects of stimulus type, visual field coverage and stimulus motion on MEG and EEG recordings. *Neuroimage* 69:223–230.

24. Busch NA, Dubois J, VanRullen R (2009) The phase of ongoing EEG oscillations predicts visual perception. *J Neurosci* 29(24):7869–76.

25. Landau AN, Schreyer HM, Van Pelt S, Fries P (2015) Distributed Attention Is Implemented through Theta-Rhythmic Gamma Modulation. *Curr Biol* 25(17):2332–2337.

26. van Dijk H, Schoffelen J-M, Oostenveld R, Jensen O (2008) Prestimulus oscillatory activity in the alpha band predicts visual discrimination ability. *J Neurosci* 28(8):1816–23.

27. Tavor I, et al. (2016) Task-free MRI predicts individual differences in brain activity during task performance. *Science* 352(6282):216–20.

28. Cole MW, Ito T, Bassett DS, Schultz DH (2016) Activity flow over resting-state networks shapes cognitive task activations. *Nat Neurosci* 19(12):1718–1726.

29. Rabiner L., Juang BH (1986) An introduction to hidden Markov models. *IEEE ASSP Mag* 3(January):4–16.

30. Baker AP, et al. (2014) Fast transient networks in spontaneous human brain activity. *Elife* 3. doi:10.7554/eLife.01867.

31. Vidaurre D, et al. (2016) Spectrally resolved fast transient brain states in electrophysiological data. *Neuroimage* 126:81–95.

32. Vidaurre D, et al. (2017) Discovering dynamic brain networks from big data in rest and task. *Neuroimage*. doi:10.1016/j.neuroimage.2017.06.077.

33. Vidaurre D, et al. (2017) Spontaneous cortical activity transiently organises into frequency specific phase-coupling networks. *bioRxiv*:150607.

34. Varga AP, Moore RK (1990) Hidden Markov model decomposition of speech and noise. *International Conference on Acoustics, Speech, and Signal Processing* (IEEE), pp 845–848.

35. Eddy SR (1998) Profile hidden Markov models. *Bioinformatics* 14(9):755–763.

36. Hirschmann J, Schoffelen JM, Schnitzler A, van Gerven MAJ (2017) Parkinsonian rest tremor can be detected accurately based on neuronal oscillations recorded from the subthalamic nucleus. *Clin Neurophysiol* 128(10):2029–2036.

37. Popov T, Kastner S, Jensen O (2017) FEF-Controlled Alpha Delay Activity Precedes Stimulus-Induced Gamma-Band Activity in Visual Cortex. *J Neurosci* 37(15):4117–4127.

38. van Kerkoerle T, et al. (2014) Alpha and gamma oscillations characterize feedback and feed-forward processing in monkey visual cortex. *Proc Natl Acad Sci U S A* 111(40):14332–14341.

39. Bastos AM, et al. (2015) Visual areas exert feedforward and feedback influences through distinct frequency channels. *Neuron* 85(2):390–401.

40. Michalareas G, et al. (2016) Alpha-Beta and Gamma Rhythms Subserve Feedback and Feedforward Influences among Human Visual Cortical Areas. *Neuron* 89(2):384–397.

41. Jensen O, Mazaheri A (2010) Shaping Functional Architecture by Oscillatory Alpha Activity: Gating by Inhibition. *Front Hum Neurosci* 4:186.

42. Jensen O, Kaiser J, Lachaux J-P (2007) Human gamma-frequency oscillations associated with attention and memory. *Trends Neurosci* 30(7):317–324.

43. Klimesch W (2012) α-band oscillations, attention, and controlled access to stored information. *Trends Cogn Sci* 16(12):606–17.

44. Tallon-Baudry C, Bertrand O, Hénaff MA, Isnard J, Fischer C (2005) Attention modulates gamma-band oscillations differently in the human lateral occipital cortex and fusiform gyrus. *Cereb Cortex* 15(5):654–662.

45. Vidaurre D, Smith SM, Woolrich MW (2017) Brain network dynamics are hierarchically organized in time. *Proc Natl Acad Sci*:201705120.

46. Cabral J, et al. (2017) Cognitive performance in healthy older adults relates to spontaneous switching between states of functional connectivity during rest. *Sci Rep* 7(1). doi:10.1038/s41598-017-05425-7.

47. Northoff G, Qin P, Nakao T (2010) Rest-stimulus interaction in the brain: a review. *Trends Neurosci* 33(6):277–284.

48. Cole MW, Bassett DS, Power JD, Braver TS, Petersen SE (2014) Intrinsic and Task-Evoked Network Architectures of the Human Brain. *Neuron* 83(1):238–251.

49. Smith SM, et al. (2009) Correspondence of the brain's functional architecture during activation and rest. *Proc Natl Acad Sci* 106(31):13040–13045.

50. Finn ES, et al. (2015) Functional connectome fingerprinting: Identifying individuals using patterns of brain connectivity. *Nat Neurosci* 18(11):1664–1671.

51. Lewis CM, Bosman CA, Womelsdorf T, Fries P (2016) Stimulus-induced visual cortical networks are recapitulated by spontaneous local and interareal synchronization. *Proc Natl Acad Sci* 113(5):E606–E615.

52. Fox MD, Snyder AZ, Zacks JM, Raichle ME (2006) Coherent spontaneous activity accounts for trial-to-trial variability in human evoked brain responses. *Nat Neurosci* 9(1):23–25.

53. Fox MD, Snyder AZ, Vincent JL, Raichle ME (2007) Intrinsic Fluctuations within Cortical Systems Account for Intertrial Variability in Human Behavior. *Neuron* 56(1):171–184.

54. Dijk H van, Schoffelen J-M, Oostenveld R, Jensen O (2008) Prestimulus Oscillatory Activity in the Alpha Band Predicts Visual Discrimination Ability. *J Neurosci* 28(8):1816–1823.

55. Hanslmayr S, et al. (2007) Prestimulus oscillations predict visual perception performance between and within subjects. *Neuroimage* 37(4):1465–1473.

56. Jones SR, et al. (2010) Cued Spatial Attention Drives Functionally Relevant Modulation of the Mu Rhythm in Primary Somatosensory Cortex. *J Neurosci* 30(41):13760–13765.

57. Linkenkaer-Hansen K, Nikulin V V., Palva S, Ilmoniemi RJ, Palva JM (2004) Prestimulus Oscillations Enhance Psychophysical Performance in Humans. *J Neurosci* 24(45):10186–10190.

58. Lange J, Halacz J, van Dijk H, Kahlbrock N, Schnitzler A (2012) Fluctuations of Prestimulus Oscillatory Power Predict Subjective Perception of Tactile Simultaneity. *Cereb Cortex* 22(11):2564–2574.

59. Baumgarten TJ, Schnitzler A, Lange J (2015) Beta oscillations define discrete perceptual cycles in the somatosensory domain. *Proc Natl Acad Sci* 112(39):12187–12192.

60. Oostenveld R, Fries P, Maris E, Schoffelen J-M (2011) FieldTrip: Open Source Software for Advanced Analysis of MEG, EEG, and Invasive Electrophysiological Data. *Comput Intell Neurosci* 2011:1–9.

61. Hyvarinen A (1999) Fast and robust fixed-point algorithms for independent component analysis. *IEEE Trans Neural Networks* 10(3):626–634.

62. Nolte G (2003) The magnetic lead field theorem in the quasi-static approximation and its use for magnetoencephalography forward calculation in realistic volume conductors. *Phys Med Biol* 48(22):3637–3652.

63. Holmes CJ, et al. (1998) Enhancement of MR images using registration for signal averaging. *J Comput Assist Tomogr* 22(2):324–333.

64. Fischl B, Sereno MI, Dale AM (1999) Cortical Surface-Based Analysis. *Neuroimage* 9(2):195–207.

65. Gramfort A, et al. (2014) MNE software for processing MEG and EEG data. *Neuroimage* 86:446–460.

66. Van Veen BD, Buckley KM (1988) Beamforming: a versatile approach to spatial filtering. *IEEE assp Mag* 5(2):4–24.

67. Lancaster JL, et al. (1997) Automated labeling of the human brain: A preliminary report on the development and evaluation of a forward-transform method. *Human Brain Mapping*, pp 238–242.

68. Colclough GL, Brookes MJ, Smith SM, Woolrich MW (2015) A symmetric multivariate leakage correction for MEG connectomes. *Neuroimage* 117:439–448.

69. Thomson D (1982) Spectrum estimation and harmonic analysis. *Proc IEEE* 70(9):1055–1096.